International Conference on Advances in Structural and Geotechnical Engineering

ICASGE'17

27-30March 2017, Hurghada, Egypt

SHEAR BEHAVIOUR OF SHCC DRY JOINTS IN PRECAST CONCRETE CONSTRUCTION

M. A. KASSEM, T. F. EL-SHAFIEY, M. HUSSEIN, H. M. AFEFY AND A. HASSAN

ABSTRACT

Shear key is commonly used to connect two separate precast components in order to increase the interfacial shear resistance of the joint. The small dimensions of the shear key do not permit providing conventional reinforcement; consequently its ability to transmit shear force is mainly dependent on the mechanical properties of the used concrete. The enhanced shear capacity arising from using high strength concrete is always on the expense of the developed ductility. This paper presents an experimental and analytical investigation on the strength of the shear key connection in precast concrete construction that made of Strain Hardening Cementitious Composites (SHCCs). Thus, using of SHCCs, with their superior tensile strength and ductile behavior, in the shear key zone, not only improve both joint strength and ductility but also, control the cracks propagation as well. The shear keys test specimens were selected in the form of trapezium that is made up with 3 different key's angles. The main parameters for tests were the inclination angle of the shear key and the level of the confining stress. All specimens are tested using the "push-off" method in order to obtain the ultimate shear capacity of the connection. Accordingly, the overall shear behavior including ultimate shear resistance, crack pattern and modes of failure of the joints and the manifested slip were investigated. It was found that all tested specimens experienced shearing failure. However, SHCC shear keys are found to have more ductile mode of failure compared with that exhibited by normal strength concrete (NSC) specimen. It could be concluded that the use of SHCC significantly improves both the shear strength and the corresponding ductility of the joint. Based on the experimental results a simple analytical model is proposed for estimating the ultimate shear capacity of SHCC dry joint. The proposed analytical model showed good agreement with the experimental findings.

Keywords: Shear key; Stain Hardening Cementitious Composites (SHCC); shear strength; precast joints; external prestressing.

INTRODUCTION

Nowadays, the demand for rapid assembly, high quality control, low construction cost, and mitigated environmental disturbance for bridge construction made the precast bridge construction technique the best choice for many bridge projects worldwide. Even though, the joints between the adjacent parts in the segmental concrete construction present locations of discontinuity that could affect the overall structural performance of precast concrete segmental bridges. Many researches have been carried out on the precast concrete deck bridges with dry joints and provided with external tendons in order to overcome their drawbacks associated with the deficient shear capacity and the corrosion of pre-stressed tendons [1]. The shear capacity of the dry joints is a summation of two qualitatively and quantitatively different components [1-6]. The first component is the frictional resistance that arises when two flat and compressed surfaces attempt to slide one against the other. This resistance is proportional to the acting compressive stress and the corresponding friction coefficient (μ), which can be slightly improved by adding a resin material between segments [7-9]. While the second component is the shear strength of the shear keys provided by surface area that called cohesion (c), which is mainly dependent on the properties of mix forming the two surfaces. Normal Strength Concrete (NSC) is known to have low tensile strength and strain that affect negatively on the key shear capacity. So, using of fibrous concrete with its enhanced tensile strength may improve the shear capacity of the shear key depending on the type and the used fiber volumetric ratio [10]. Strain hardening Cementitious composites (SHCC) is a special category of the new generation of high-performance fiber reinforced cementitious composites, where the use of fibers in the

absence of coarse aggregate enhance significantly its ultimate tensile strength and stain [11-13]. SHCC has high tensile ductility, deformation compatibility with existing concrete and self-controlled micro-crack width that lead to their superior durability characteristics under various mechanical and environmental loading conditions such as fatigue, freezing, chloride exposure and drying shrinkage [14-16]. The idea of the present work is based on utilizing the beneficial properties of a strain harding cementitious composites (SHCC) in order to improve the shear behavior of dry joints.
In this paper, an experimental program is conducted in order to verify the adequacy of SHCC dry joints considering different shapes of shear key, type of concrete and initial prestressing level. Discussion of the results is presented in terms of mode of failure, cracking pattern, crack opening, load-shear slip relationships, strain development and toughness.

Experimental work program

Test specimens

A total of nine specimens were fabricated and tested under the push-off test method. The specimens were divided into three groups (I, II and III) along with two reference specimens (S-F and S-C) were prepared to quantify the friction and cohesion between the adjacent parts. Specimen S-F has been fabricated without shear key (flat joint) to quantify the frictional shear resistance between the adjacent parts. Accordingly, the friction coefficient of the joint, μ_1, can be determined properly. On the other hand, specimen S-C was configured in order to determine the cohesion component, c. The remaining seven specimens were divided into three groups. The first group consisted of two specimens that were made of different mixes; namely, Normal Strength Concrete (NSC), and SHCC. While all specimens of the second group GII and the third group GIII were made of SHCC material. The main testing parameter of the second group GII was the inclination angle of shear key (45, 60, and 90^o). While the three specimens of the last group GIII were tested under different confining pressure; 0.5, 2.0, and 3.0 MPa. The dimensions and configurations of the tested specimens for the flat and the single-keyed joints were chosen to satisfy the minimum dimensions of AASHTO [2] requirements, refer to Figs. 1 and 2. All test specimens had the same thickness of 100 mm. Table 1 summarizes the characteristics of all test specimens.

Each specimen was divided into three panels; namely A, B and C as depicted in Fig. 3. Thus, each specimen was cast in two phases; the panels A and B were cast in the first phase and afterward, when these panels were hardened, the casting of the central panel C took place. In this way, the sides of the lateral female panels were used as a side of the molds for the central panels. Fig. 3 shows the surface texture of the lateral panel, which provided with a thin aluminum sheet before molding the lateral panels. At the age of 28 days, each specimen was assembled using four (two per side) externally pre-stressed stainless steel bars of 12 mm diameter. The stainless steel bars were accommodated into two steel plates of 20 mm thickness at both sides of the specimen as depicted in Fig. 1(b). The prestressing effect was conducted using end nuts at both ends of each bar as shown in Fig. 1. The contribution of cohesion in the shear capacity was evaluated by testing of specimen S-C where no friction force was developed due to the using of 5 mm thickness foam as a separate material between the segments as shown in Fig. 4. In other words, the load was completely transferred to the lateral panels by bearing.

Material Properties

Material Properties

Two different mixes were used to cast the test specimens. The first mix of the NSC was proportioned for 28-day cylindrical compressive strength of 30 MPa. Mix proportions of the used concrete are illustrated in Table 2. In addition, the mix proportions of the SHCC castellated specimens are listed in Table 2. For the SHCC material, the water-to-binder ratio (W/B) was kept 0.20. Ordinary Portland cement having a density of 3.14 g/cm^3 was used, and 15% of the design cement content was replaced by silica fume. Quartz sand with a diameter less than 0.5 mm was used as a fine aggregate. High strength Polypropylene (PP) fiber was chosen for SHCC and its volumetric ratio was 2.0%. The average cylindrical compressive strength at the age of 28 days was designed to be 50 MPa.
The actual average strength of NSC and SHCC was determined as summarize in Table 3. Standard test method for both compressive and tensile strength of cylindrical specimens was carried out according to ASTM C39 and C496; Table 3 summarizes the obtained materials characteristics. In order to determine the mechanical properties of the used high-strength stainless steel of 12 mm diameter bars, tensile tests

were performed on three typical specimens. The average ultimate strength was 980 MPa, while the corresponding ultimate strain was 0.5%.

Test setup and procedure

In order to simulate the prestressing effect in the segmental concrete bridges application; a uniform confining pressure was employed by a tightening torque applied to the nuts of the externally prestressed bars. One strain gauge was mounted on every stainless steel bar in order to monitor the bar tensile strain. Thus, the required developed strain corresponding to specific lateral pressure can be measured and adjusted until the design value was attained. The panels were placed on support plates mounted on steel rollers. In this way, the supports only restricted vertical displacements. A hydraulic actuator applied the load on the top of the central panel, while a load cell of 500 kN capacity was used to measure the acting load. Vertical shear slip at the middle of the intermediate panel was measured during the test using LVDTs (stroke = 50mm, sensitivity = 0.005mm). An automatic data acquisition system was used to record and store the reading of vertical load, displacements and the developed normal strain on the external prestressed steel bars. The instrumentation used to monitor the behavior of the specimens during testing is shown in Fig 1.

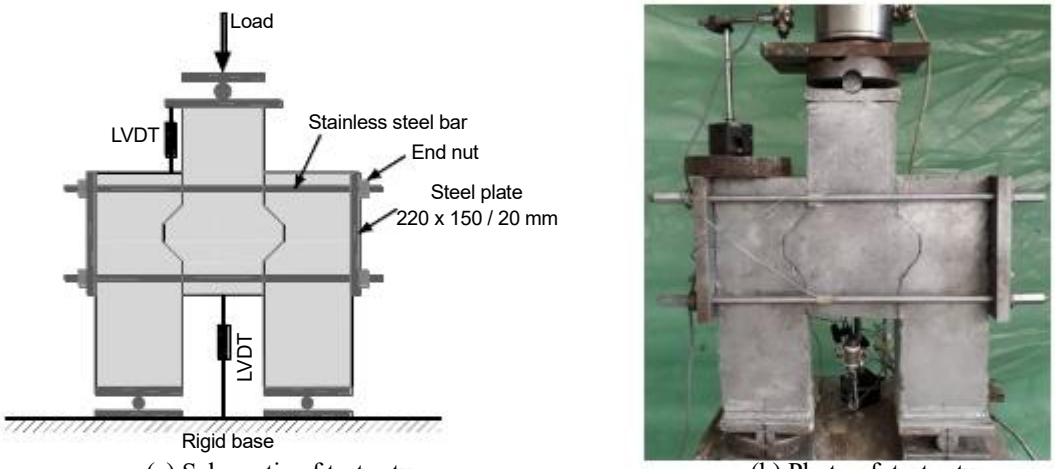

(a) Schematic of test setup (b) Photo of test setup

Fig. 1: Push-off test setup and instrumentations.

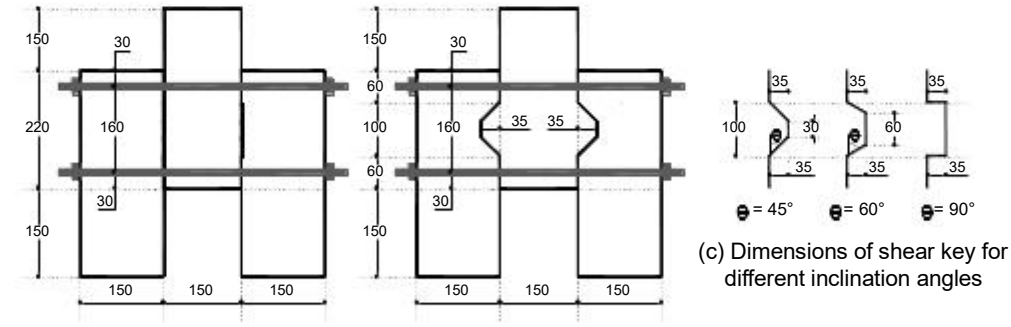

(a) Dimensions of specimen S - F (b) Dimensions of single keyed joint

(c) Dimensions of shear key for different inclination angles

Fig. 2 Details of test specimens.

(a) Ply wood form of specimens

(b) Panels A and B after casting

(c) Mold of panel C

(d) Panel C after casting

Fig. 3 Fabrication process of test specimens

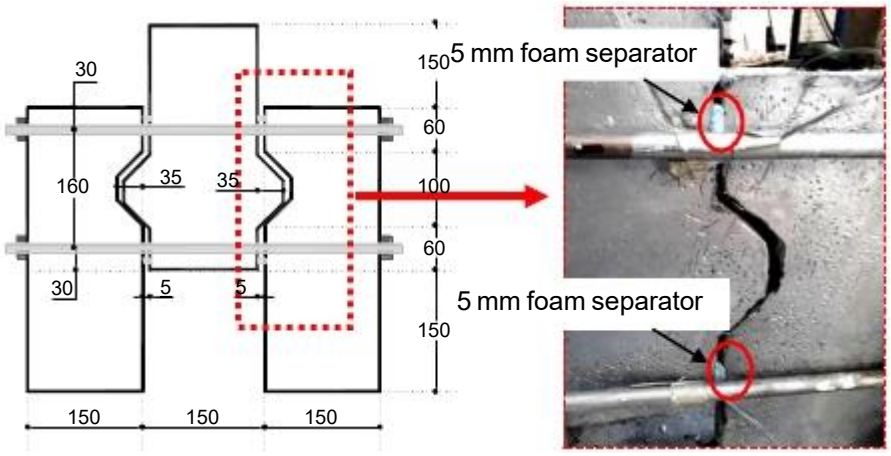

Fig. 4 Details of cohesion test specimen S - C

Table 1 : Test matrix

Group No	Specimen	Material type	Inclination angle of the shear key	Initial confining stress (MPa)	Prestressing force (kN)	Objectives
Friction test	S-F*	SHCC	---	1.0	22	Determine μ1
Cohesion Test	S-C	SHCC	45	--	--	Determine c
Group (I)	N-45-1	NSC	45	1.0	22	Study the effect of material type
	S-45-1	SHCC	45	1.0	22	
Group(II)	S-60-1	SHCC	60	1.0	22	Study the effect of inclination angle
	S-90-1	SHCC	90	1.0	22	
Group (III)	S-45-0.5	SHCC	45	0.5	11	Study the effect of prestressing level
	S-45-2	SHCC	45	2.0	44	
	S-45-3	SHCC	45	3.0	66	

* Without shear key; μ1= surface friction coefficient; and c = cohesion

Table 2: Mix proportions of the used NSC and SHCC material for cubic meter

Material	Cement (kg)	Sand (kg)	Coarse aggregate (kg)	Silica fume (kg)	Fibers (kg) (volumetric ratio)	Super plasticizers (kg)	Water (kg)	Water-to-binder ratio
NSC	350	535	1279	---	---	---	175	0.50
SHCC	1342	157.9	-----	237	16.20 (2.0%)	31.6	312.1	0.20

Table 3: Summery of material test results

Material	Compressive strength (MPa)	Ultimate compressive vertical strain (%)	Ultimate compressive horizontal strain (%)	Average tensile strength (MPa)
NSC	27	0.02	0.008	2.95
SHCC	42	0.06	0.028	5.00

Test results and discussion

Flat joint test

In order to quantity the concrete-to-concrete friction coefficient, μ_1,specimen S-F was fabricated and tested. First, the specimen was subjected to 1.0 MPa confining stress and tested under vertical load (S-F-1). After that the panels of the specimen were realigned and then the confining stress was doubled and then the specimen was tested again (S-F-2). Tests were continued till the vertical slip of the central panel reached about 8.0 mm [6].

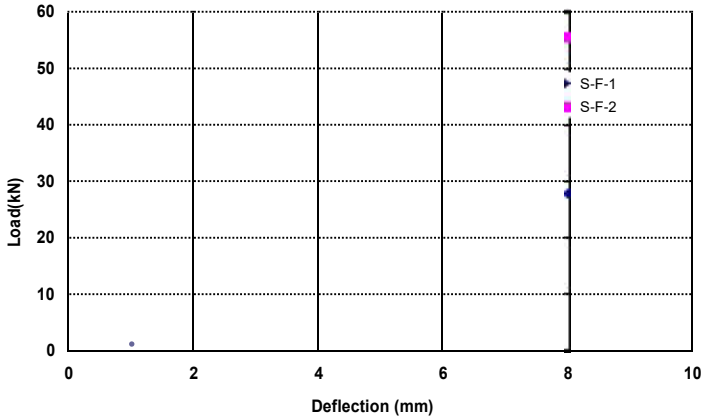

Fig. 5 Load versus shear slip of flat joint.

The shear load-vertical slip curves of the flat joint specimen are shown in Fig. 5. It can be observed that the load increases approximately linearly to the stress level at which the panels surfaces started to slip against each other. No cracks were observed on the specimen, except a small-scale grinding as evidenced by crushing concrete powder on the surface. The maximum sustained loads by specimen S-F under the two different confining stresses of 1.0 and 2.0 MPa were about 27 and 52 kN, respectively, which reveals that the capacity of flat joints linearly proportional to confining stress.

To determine the surface friction coefficient, μ, a previous expression was proposed for the ultimate shear capacity of flat joints in terms of the confining pressure neglecting the effect of concrete strength AASHTO [2]. The shear capacity of dry flat joints can be estimated as:

$$V_{joint} = \mu_1 A_{joint} \sigma_n \quad (1)$$

Where μ_1 is the friction coefficient, σ_n is the lateral confining stress, and A_{joint} is the area of the contact surface between segments. Accordingly, the mean friction coefficient obtained from this test had a value approximately equal to 0.6 which is consistent with AASHTO [2] provisions.

Single-keyed joints test

The obtained experimental results of the single-keyed specimens are presented and subsequently discussed in terms of the observed mode of failure, ultimate loads, load-shear slip behavior, and cracking behavior.

Ultimate shear capacity

Table 4 summarizes the recoded ultimate loads for all specimens. The experimental results reported in Table 4 show that the failure load of the control specimen N-45-1 was 180kN, which represents the minimum load carrying capacity achieved by single keyed specimens. On the other hand the use of SHCC was able to increase the ultimate load of specimen S-45-1 to 300 kN, approximately 67% higher than that achieved by specimen N-45-1. This can be attributed to the enhanced characteristics of the SHCC in both compression and tension. Moreover, it could be seen that the shear capacity of the SHCC specimens was significantly increased with the increase of prestressing level. The greatest increase in the ultimate load over the control specimen N-45-1 was obtained by specimen S-45-3 that is about 114%. Experimental results reported in Table 4 indicate that a slight increase in the ultimate load was achieved within the increase in the inclination angle of shear key. This is because the increase of the inclination angle resulted in a decrease in the slipping force which reduces the prestressing effect.

The reverse capacity of the tested specimens represented by the difference between ultimate and cracking loads is given in Table 4. It is obvious that the reverse capacity increased as the joint type changed from NSC to SHCC. The significant increase in the post-cracking capacity may be attributed to the addition of fibers in SHCC mix. Fibers can bridge stress on the crack surface of the SHCC similar to conventional shear reinforcement. Consequently, the reverse capacities of SHCC specimens increased. Specimen S-45-1 achieved a reverse capacity of 165 kN, 135% higher than that of N-45-1. This means that SHCC gives enough warning before failure in comparison with NSC.

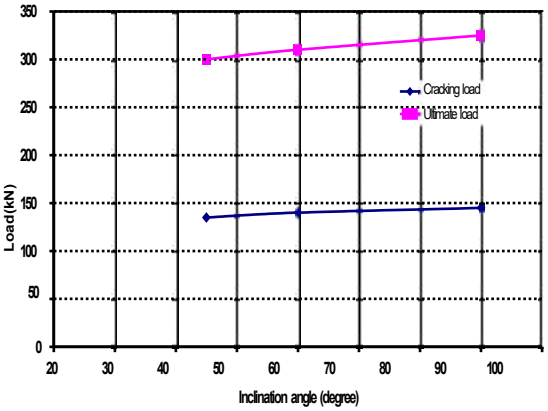

Fig. 6 Loads versus inclination angle. (SHCC specimens)

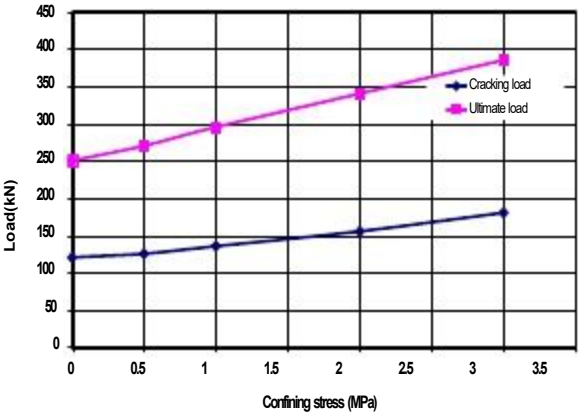

Fig. 7 Loads versus prestressing level. (SHCC specimens)

Cracking behavior

Fig. 8 shows the cracking sequence of the tested shear key specimens. At approximately 45% of the ultimate load of SHCC shear key specimen and 65% of the ultimate load of NSC specimen, a single curvilinear crack (S-crack) was initially formed at the bottom corner of the shear key and propagated sideways and upward at approximately 45º to the horizontal. Later on, S-crack tends to stop propagating; since the rotation of the shear key decreases the stresses at the base of shear key. With further shear loading approaching the ultimate load, intensive multiple diagonal cracks (M-cracks) were observed at the root of the shear key. Finally, after crushing of compression struts between M-cracks, the specimen failed due to shearing-off. This is coincident with the observations of Kaneko et al. [3] in their tests.

Table 5 shows the results of crack width visual inspection, taken when the specimens were subjected to moderate (140 kN) and high (170 kN) loads, as well as after being subjected to the ultimate load achieved. The first crack was observed in specimen N-45-1 when the applied load reached about 110 kN, 65% of its ultimate capacity. With further loading, the major crack width was increased up to 0.50 mm approaching the complete failure of the specimen. A considerable enhancement in the cracking load of specimen S-45-1 was obtained, that was about 135 kN, which is 22% more than that of specimen N-45-1 accompanying by 40% reduction in major crack with, which declares that the use of SHCC can effectively improve the cracking behavior of the shear key. Fig. 6 shows that increasing the inclination angle of the shear key decreases the slipping force acting at the base of the shear key, consequently, the cracking loads of specimens S-60-1 and S-90-1 was about 140 and 145 kN, respectively which is higher than the load achieved by specimen S-45-1, by about 3.7 % and 7 %, respectively. In addition, increasing the applied prestressing level, increased the cracking loads of specimens S-45-0.5, S-45-1, S-45-2, and S-45-3 by about 4, 12, 25, and 50%, respectively, compared with that of specimen S-C which was tested in order to obtain the cohesion capacity of shear key, refer to Fig. 7.

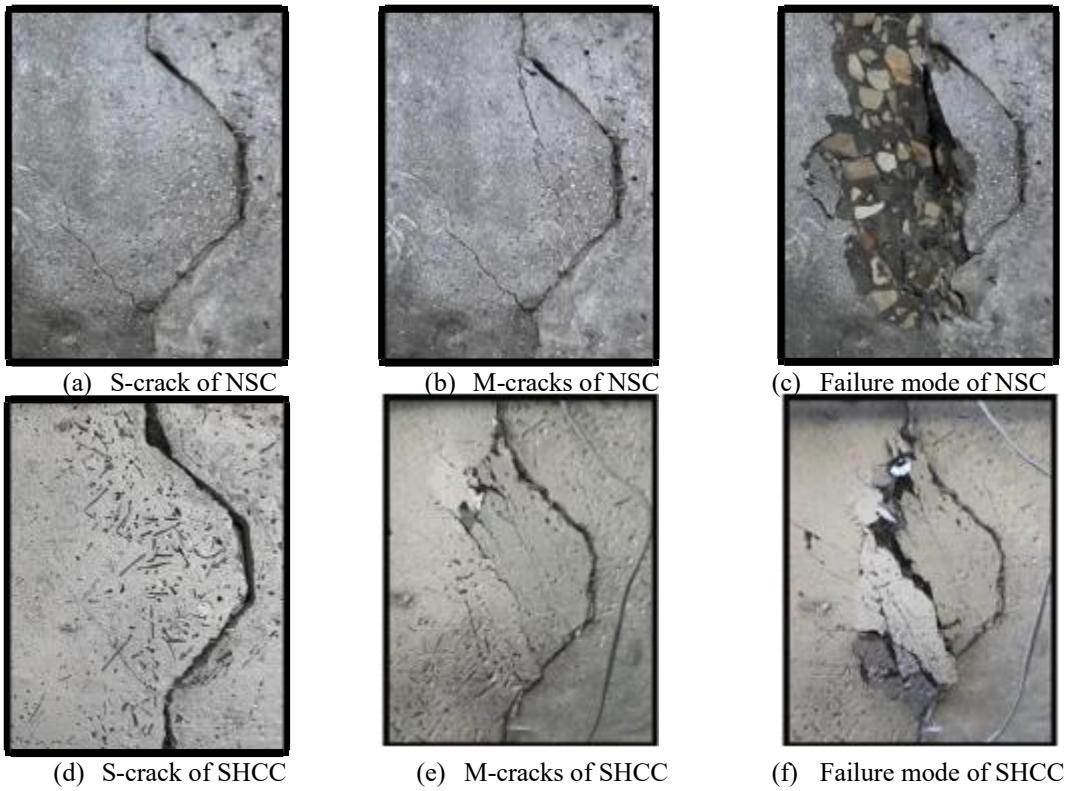

(a) S-crack of NSC (b) M-cracks of NSC (c) Failure mode of NSC

(d) S-crack of SHCC (e) M-cracks of SHCC (f) Failure mode of SHCC

Fig. 8 Cracks propagation and modes of failure of shear key.

Table 4: Summery of experimental test results

Group	specimen	P_{cr} (kN)	P_u (kN)	P_r (kN)	Δ_u (mm)	Mode of failure
Friction test	S-F	---	29	--	9.00	Sliding
Cohesion test	S-C	120	245	125	2.28	Shear
Group 1	N-45-1	110	180	70	2.97	Shear
	S-45-1	135	300	165	2.02	Shear
Group 2	S-60-1	140	310	170	1.70	Shear
	S-90-1	145	325	180	1.65	Shear
Group 3	S-45-0.5	125	270	145	1.73	Shear
	S-45-2	150	345	195	1.92	Shear
	S-45-3	180	385	205	2.05	Shear

P_{cr}=cracking load, P_u=ultimate load, P_r= reverse capacity = P_u - P_{cr} ; Δ_u=ultimate deflection and

Table 5: Maximum crack width at 140 kN, 170 kN and at ultimate load.

Group	Specimen	Maximum crack width developed in key		
		At 140 kN (mm)	At 170 kN (mm)	At ultimate (mm)
Group 1	N-45-1	0.30	0.45	0.50
	S-45-1	0.05	0.10	0.30
Group 2	S-60-1	--	0.05	0.30
	S-90-1	--	0.05	0.25
Group 3	S-45-0.5	0.10	0.15	0.35
	S-45-2	--	0.05	0.30
	S-45-3	--	---	0.30

Load - shear slip relationship

Fig. 10 shows the relationships between the applied load and the corresponding shear-slip for all test specimens of groups I, II, and III. With regard to specimen N-45-1 that was made of NSC, it can be seen that the load increased continuously till the cracking load. The formation of the crack was accompanied with dilation in the specimen. Consequently, the frictional resistance from the flat portion below the key was greatly reduced at this stage, which explains the reduction in shear stiffness after the formation of the crack at the root of the key. At the maximum load level, the specimen failed due to the crushing of compression strut followed by shearing-off of the key. This was accompanied by a sudden and large slip between the two parts of the specimen. Whereas, the SHCC specimens behaved a similar trend till cracking beyond which the residual stiffness (stiffness after cracking) of SHCC specimens was greater than that of NSC specimen. This is attributed to the bridging effect of fibers which enhances the energy absorption capacity. Furthermore, after the SHCC specimens reached their ultimate capacity, and contrary to the observed behavior of NSC specimen, the high post-cracking tensile deformability and resistance of SHCC avoid the occurrence of premature fracture failure, the load drops gradually from the peak to a load level round that carried by friction. This means that failure in SHCC specimens was more ductile than that of NSC specimen. Also, as can be seen in Fig. 10 the shear stiffness of SHCC specimens increased as the confining pressure increased. Moreover, with the increase of the slope angle of the shear key the shear stiffness of the joint increased.

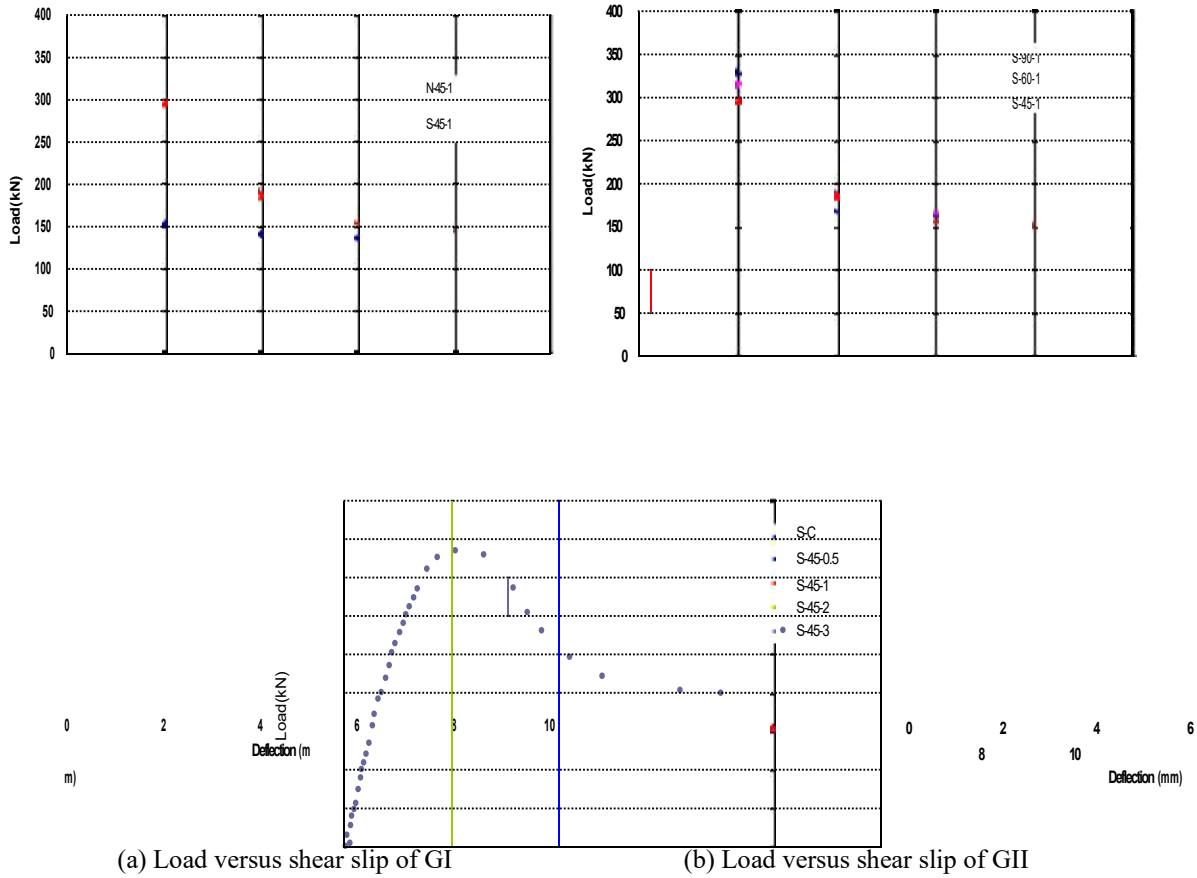

(a) Load versus shear slip of GI (b) Load versus shear slip of GII

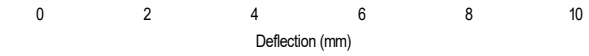

(c) Load versus shear slip of GIII

Fig. 10 load versus shear-slip of tested specimens

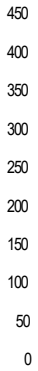

Shear strength of SHCC dry Joints

Shear strength of dry joints with castellated keys comprises two contributions. The first contribution is that the friction resistance starts when two flat and compressed surfaces attempt to slide against each other. This resistance is proportional to the actuating compression and the corresponding proportionality factor, which is the friction coefficient, μ_1. The second contribution is the support effect of the castellated shear keys. These keys permit shear transfer when they are in contact with each other; they behave like small corbels. The shear strength of the keys by surface area is called cohesion.

AASHTO [4] gives the following formula for estimating the shear capacity of single key joints applying a reduction factor to the results, $\phi = 0.75$.

$$V_u = A_k \sqrt{f'_c}.(0.2048.\sigma_n + 0.9961) + \mu_1 A_{sm}.\sigma_n \qquad (2)$$

Where: A_k = base areas of all keys in the failure plane; f_c' = compressive strength of concrete (MPa); σ_n = effective normal compressive stress in concrete at the centroid of the cross section (MPa); and A_{sm} = area of contact between smooth surfaces on the failure plane.

The shear strengths obtained from the experimental work were compared with the results of AASHTO formula, which are given in Table 5. Applying the AASHTO formula to specimen N-45-1 that was made of normal strength concrete gives a good prediction of shear strength. On the other hand the AASHTO values are conservative with the SHCC specimens, this can be explained by the fact that ASSHTO formula was derived from the theoretical and experimental work of single-keyed joints made of ordinary concrete. The addition of fibers to the SHCC mix proportions has been shown to enhance shear resistance and ductility of SHCC joints. Fibers increase shear strength by providing post-cracking diagonal tension resistance, similar to the effect of steel reinforcement. AASHTO does not consider the contribution of fibers to shear strength; consequently the ASSHTO formula underestimates the shear capacity of joints. Since the contribution of fibers to the joint shear strength is significant as confirmed by this study, it is recommended that the AASHTO equation for key precast segment joints should be modified to take into consideration the contribution of fibers to shear strength. Based on the concepts presented JSCE [15], the nominal shear strength of SHCC dry joint may be obtained by the addition of fiber contribution to the shear strength. This is expressed in following equation.

$$V_u = \left[A_k \sqrt{f'_c}\,(0.2048.\sigma_n + 0.9961) \right] + \mu_1 A_{sm}.\sigma_n + f_{vd}.A_k / 1.15 \tan\beta \qquad (3)$$

Where: f_{vd} = the tensile yield strength of SHCC; β = angle of the diagonal crack to the member axis β = 45 º

In order to examine the validity of the proposed procedure, a comparison of the proposed analytical approach with the experimental results is shown in Fig.11. It can be concluded that, the proposed formula is in good agreement with the test results.

Table 5: Verification of the proposed equation

Specimen	P_u Experimental (kN)	AASHTO		Proposed	
		P_u (kN)	1.3 xAASHTO Experiment al	P_u (kN)	Proposed Experiment al
N-45-1	180	139	1.00	--	--
S-C	245	132	0.70	255	1.04
S-45-0.5	270	152	0.73	279	1.03
S-45-1	300	173	0.75	304	1.01
S-45-2	345	215	0.81	352	1.02
S-45-3	385	256	0.86	401	1.04
S-60-1	310	173	0.72	304	0.98
S-90-1	325	173	0.69	304	0.94

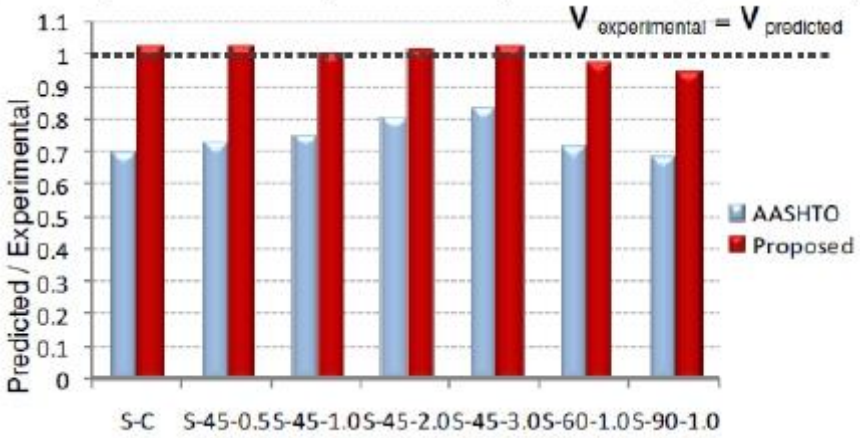

Fig. 11 Comparison of the proposed analytical approach with the experimental results

CONCLUSIONS

An experimental program was carried-out in order to evaluate the structural performance of the SHCC dry joints. Based on the experimental investigation, the following conclusions can be drawn:

1- The use of SHCC in dry joints effectively enhanced the failure mode with a more ductile response in comparison with NSC.
2- The utilization of the SHCC in dry joints provided a significant structural enhancement in the load carrying capacity which increased by about 67% compared to the NSC joint. Furthermore a remarkable improvement in the shear stiffens was obtained.
3- A great enhancement in the post-cracking behavior was recorded with the use of SHCC in the dry joints. The reverse capacity of SHCC increased to 122 % of cracking load which is 1.35 times higher than that achieved by the NSC. Accordingly, the SHCC gives enough warning before failure in comparison with NSC.
4- The variation of the inclination angle of the SHCC-shear key slightly affects the shear stiffness and the load carrying capacity of the joints.
5- The achieved cracking load, ultimate load and the shear stiffness of the SHCC specimens increased with the increase of the initial confining pressure.
6- The proposed analytical model is capable of predicting the ultimate shear capacity of SHCC dry joints. Excellent agreement was established between the predicted values using the proposed model and those recorded experimentally.

ACKNOWLEDGMENTS

This paper is a part of an ongoing PhD thesis of the last author that supervised by the rest of co-authors. The PhD thesis presents a new generation of high performance composite precast bridge deck.

REFERENCES

[1] Foure, B., Bouafia, Y., Soubret, R., Thomas, P. (1993). ―Shear test on keyed joints between precast segments.‖ Proc., Workshop on Behaviour of External Prestressing in Structures, Association Française pour la Construction (AFPC), 297–319.

[2] Ramos, G., and Aparicio, A. C. (1996). ―Ultimate analysis of monolithic and segmental externally prestressed concrete bridges.‖ J. Bridge Eng., 10.1061/(ASCE)1084-0702(1996)1:1(10), 10–17.

[3] Rombach, G. A. (2004). ―Dry joint behavior of hollow box girder segmental bridges.‖ Proc., Int. fib Symp.—Segmental Construction in Concrete, International Federation for Structural Concrete (fib), Lausanne, Switzerland.

[4] AASHTO. (2003). Guide specifications for design and construction of segmental concrete bridges: 2003 interim revisions, 2nd Ed., Washington, DC.

[5] Yang, K. H., Sim, J. I., Kang, J. H., and Ashour, A. F. (2012). ―Shear capacity of monolithic concrete joints without transverse reinforcement.‖ Mag. Concr. Res., 64(9), 767–779.

[6] Turmo, J., Ramos, G., and Aparicio, A. C. (2012). ―Towards a model of dry shear keyed joints: Modelling of panel tests.‖ Comput. Concr., 10(5), 469–487.

[7] Zhou, X., Mickleborough, N., and Li, Z. (2005). ―Shear strength of joints in precast concrete segmental bridges.‖ ACI Struct. J., 102(1), 3–11.

[8] Issa, M. A., and Abdalla, H. A. (2007). ―Structural behavior of single key joints in precast concrete segmental bridges.‖ J. Bridge Eng., 10.1061/ (ASCE)1084-0702(2007)12:3(315), 315–324.

[9] Maalej, M., Hashida, T., and Li, V.C. (1995). ―Effect of Fiber Volume Fraction on the Off-Crack-Plane Fracture Energy in Strain-Hardening Engineered Cementitious Composites‖, J. Amer. Ceramics Soc., Vol. 78, No. 12, pp. 3369-3375.

[10] Fischer, G., and Li, V.C. (2005) ―Effect of fiber reinforcement on the response of structural members‖, Engineering Fracture Mechanics, 74.

[11] Afefy H.M., Kassem N.M. and Hussein M. (2015). ―Enhancement of flexural behavior of CFRP-strengthened reinforced concrete beams using engineered cementitious composites transition layer‖, Structure and Infrastructure Engineering, UK Vol. 11, No. 8, pp. 1042–1053.

[12] Hussein M., Kassem N.M., and Hassan A. (2015) ―An Innovative Efficient Strengthening For Reinforced Low Strength Concrete Cantilever Slabs‖ (IOSR-JMCE), Volume 12, Issue 5 Ver. I, PP 01-13

[13] Sahmaran, M., Li, M., and Li, V.C. (2007). ―Transport properties of engineered cementitious composites under chloride exposure‖, ACI Material Journal, 104, pp 604–611.

[14] Dhawale, A.W., and Joshi, V.P. (2013). ―Engineered cementitious composites for structural applications‖, International Journal of Application or Innovation in Engineering & Management, pp 198–205.

[15] Japan Society of Civil Engineers (2008). ―Recommendations for Design and Construction of High Performance Fiber Reinforced Cement Composites with Multiple Fine Cracks‖, series 82.

[16] Afefy H. M., Kassem N. M., Hussien M. and Taher S.F. (2016) ―Efficient strengthening of opened-joint for reinforced concrete broken slabs‖ Composite Structures, Vol. 136, February, pp. 602-615.